

In-vitro analysis of normal and aneurismal human ascending aortic tissues using FT-IR microspectroscopy

F. Bonnier^a, S. Rubin^{a,b}, L. Ventéo^c, C.M. Krishna^d, M. Pluot^c, B. Baehrel^b,
M. Manfait^{a,*}, G.D. Sockalingum^a

^a Unité MéDIAN, CNRS UMR 6142, UFR de Pharmacie, IFR 53, Université de Reims Champagne-Ardenne, 51 rue Cognacq-Jay, 51096 Reims cedex, France

^b Service de Chirurgie Thoracique et Cardiovasculaire CHU de Reims, Hôpital Robert Debré, Avenue du Général Koenig, 51092 Reims cedex, France

^c Laboratoire Central d'Anatomie et Cytologie Pathologiques, CHU de Reims, Hôpital Robert Debré, Avenue du Général Koenig, 51092 Reims cedex, France

^d Center for Laser Spectroscopy Manipal Academy of Higher Education, Manipal-576104, India

Received 9 January 2006; received in revised form 19 May 2006; accepted 19 May 2006

Available online 2 June 2006

Abstract

FTIR microspectroscopy has shown to be a proven tool in the investigation of many tissue types. We have used this spectroscopic approach to analyse structural differences between normal and aneurismal aortic tissues and also aortas from patients with congenital anomalies like aortic bicuspid valves. Spectral analysis showed important variations in amide I and II regions, related to changes in alpha-helix and beta-sheet secondary structure of proteins that seem to be correlated to structural modifications of collagen and elastin. These proteins are the major constituents of the aortic wall associated to smooth muscular cells. The amide regions have thus been identified as a marker of structural modifications related to these proteins whose modifications can be associated to a given aortic pathological situation. Both univariate (total absorbance image and band ratio) and multivariate (principal components analysis) analyses of the spectral information contained in the infrared images have been performed. Differences between tissues have been identified by these two approaches and allowed to separate each group of aortic tissues. However, with univariate band ratio analysis, the pathological group was found to be composed of samples from aneurismal aortas associated or not with an aortic bicuspid valve. In contrast, PCA was able to separate these two types of aortic pathologies. For other groups, PCA and band ratio analysis can differentiate between normal, aneurismal, and none dilated aortas from patients with a bicuspid aortic valve.

© 2006 Elsevier B.V. All rights reserved.

Keywords: FTIR microspectroscopy; Aortic tissue; Aneurysm; Aortic bicuspid valve; PCA analysis

1. Introduction

Human aneurism is a common pathology encountered daily in the cardio-vascular surgery unit. Different pathologies of the aortic wall, such as aortic ectasia, stenosis or aneurysm are known [1]. The most important corresponds to dilations with or without atheroma (accumulation of lipid, calcium, and fibrosis). The exact physiopathology of this aortic dilatation is unknown but implication of Matrix Metalloproteinases or presence of congenital valve malformation is clearly associated with pathology. Macroscopic examination confirms modifications of physical characteristics with dilation, decrease of elastance and aortic wall resistance. The development of aneurysm is

multifactorial [2–6]; the final outcome of the pathology being a rupture of aortic wall, causing the death of patient in the following minutes.

At present, the main dilemma for the surgeon is to take a decision, during a heart-surgical act, whether it is necessary to replace the ascending part of aortas at the same time. To date, there is no tool available that can help the surgeon to take the proper decision. For the patient, a second surgery and replacement of the aorta many years later, increases the risk of complications by a factor of 10 [7,8]. Therefore, development of new methods that can assist the surgeon could be very helpful and beneficial to patients.

Characterisation of the different tissue types is an important issue in view of evaluating the stage of the aortic disease and it could be in the future an important parameter of the surgical decision. Application of spectroscopic methods offers the

* Corresponding author. Tel.: +33 3 26 91 35 74; fax: +33 3 26 91 35 50.

E-mail address: michel.manfait@univ-reims.fr (M. Manfait).

possibility to analyse the structural information contained in a larger area of the tissue sample and to combine morphological and chemical information.

In this study, we make a preliminary attempt to use Fourier-transform infrared (FT-IR) microspectroscopy as an *in vitro* analytical tool for discriminating between normal and pathological human aortic tissues on the one hand, and to differentiate between the different pathological tissue types, encountered during surgery, on the other hand.

2. Material and methods

2.1. Aortic samples

Biopsies of aortic tissues obtained after surgeries were classified following the 4 different groups: normal tissues, tissues from patients with bicuspid valves, aneurismal tissues from patients without bicuspid valves, and aneurismal tissues from patient with bicuspid valves. Bicuspid aortic valve is a congenital disease with only 2 aortic leaflets instead of three normal leaflets.

Bicuspid aortic valves are often associated with moderate dilations of the ascending aorta which are more difficult to assess.

Normal tissues were obtained on heart explants after a cerebral death. The different pathological samples were conserved after surgical replacement acts of pathological aortas.

All samples were first conserved in sterile physiological serum just after surgery. Only tissue stripes of 20 mm × 8 mm size were snap-frozen in liquid nitrogen and conserved at -80°C . Infrared imaging was performed on 10 μm thick cryosections placed on infrared transparent ZnSe windows.

2.2. Infrared imaging of aortic tissue sections

Spectral images were acquired using the infrared imaging system Spotlight 300 (Perkin Elmer Life Sciences, France). Acquisition areas were disposed in the

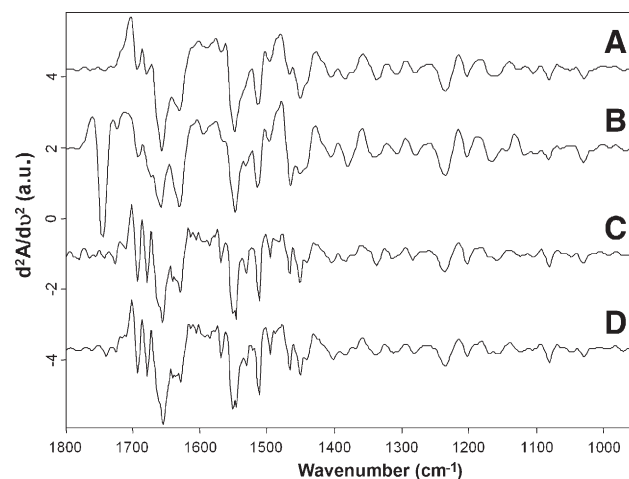


Fig. 2. Normalised second derivative of mean FT-IR spectra of aorta of four different groups of tissues. A, healthy tissue; B, tissue from patient with aortic bicuspid valve; C, aneurismal tissue from patient with normal (tricuspid) valve; and D, aneurismal tissue from patient with aortic bicuspid valve. All other conditions are as in Fig. 1.

thickness of aortas, across the three layers of the aortic wall as this is schematised in the orcein stained section which reveals the lamellar structures (Fig. 1A). IR images were acquired with a liquid nitrogen cooled mercury cadmium telluride (MCT-A) line detector composed of 16 pixel elements which can be operated either at 6.25 or 25 $\mu\text{m}/\text{pixel}$ resolution. In our study we used the highest spatial resolution. Spectral resolution was set to 4 cm^{-1} . Each absorbance spectrum composing the IR images, and resulting of 32 scans, was recorded for each pixel in the transmission mode using the Spotlight software (Perkin-Elmer). An example of an IR image based on the total absorbance and an individual pixel spectrum is shown in Fig. 1B. In these conditions, a typical area of about

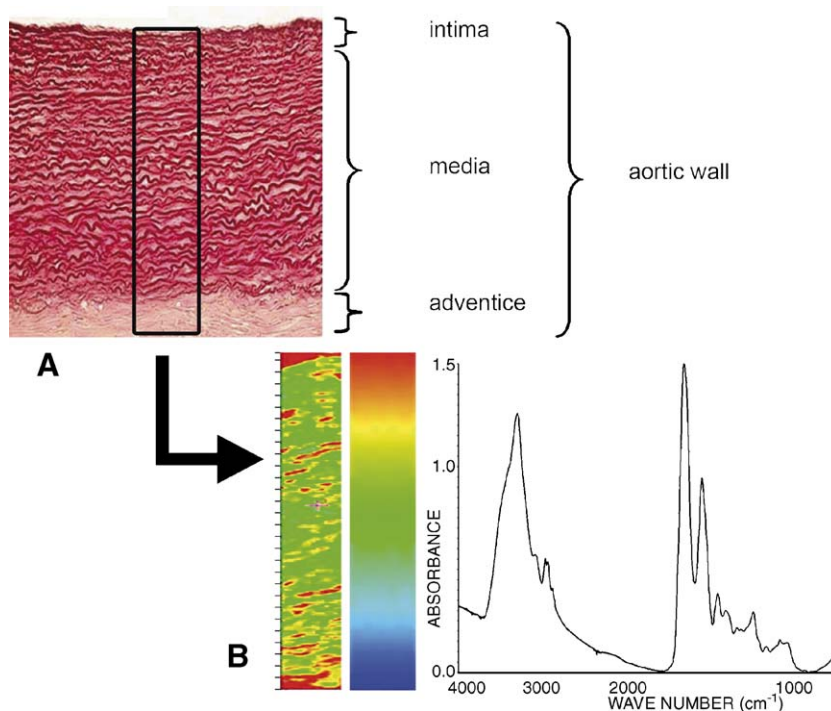


Fig. 1. (A) Histological preparation of aortic tissues. Section of orcein stained tissue showing presence of the three layers (intima, media, and adventice) of the aortic wall. The black striates present in tissue correspond to elastic fibres. (B) Total absorbance FT-IR image obtained after spectral acquisition in the selected area represented by the black triangle. The arbitrary colour scale represents total absorbance of spectra in the frequency range $4000\text{--}720\text{ cm}^{-1}$. Each pixel (size: $6.25\text{ }\mu\text{m}$) corresponds to one spectrum (32 scans at 4 cm^{-1}) which can be extracted from the image and displayed as shown.

1300 × 100 μm^2 , containing about 3000 spectra, required a recording time of about 2 h.

2.3. Data pre-processing and analysis

The Spotlight software used for acquisition was also used to pre-process the spectra. IR spectral images were produced by using the absorbance in a given frequency range, in particular here 950–1750 cm^{-1} . Spectra contained in the spectral images were in turn analysed using both a univariate approach (band ratio) and a multivariate approach based on Principal Components Analysis (PCA).

The atmospheric correction function was applied to all IR images to compensate for water vapour and contributions present in the spectra. Spectra were also subjected to a Savitzky Golay smoothing procedure (9 points). The second derivative was calculated for all spectra followed by a vector normalisation to compensate for baseline drift and sample thickness respectively (Fig. 2).

For PCA analysis we proceeded as follows: for each spectral image, about 10 zones each containing 25 spectra were selected and averaged. Mean spectra were pre-treated in the same way as explained above and were used for clustering.

Band ratio calculation: 3-D images were produced from the absorption spectra using the ratio of band areas in two regions of interest 1445–1335 and 1700–1485 cm^{-1} . Data from spectral images were further assessed by calculating the ratio (R) of band areas from the second derivative spectra of the protein absorption region: 1667–1643 over 1642–1628 cm^{-1} .

3. Results and discussion

The aortic tissue is composed of three layers (internal to external): the intima, the media and the adventice. The intima, in contact with blood, is a single layer of endothelial cells; the media, which is more implicated in aortic pathologies, is composed of concentric cylinders of smooth muscular cells associated with fibres of collagen and elastin; and the adventice, the most external layer, is composed of connective tissue with small vessels for aortic wall vascularisation. This last layer is elastic but with good resistance properties.

The infrared spectrum represents the global molecular composition of the studied tissue and reflects here the aortic wall composition at a given spatial position (Fig. 1B). The most important constituents are fibrous proteins like elastin and collagen. The 1800–950 cm^{-1} frequency range contains the major part of the information coming from these two proteins together with contributions from other cells and tissues molecular components like polysaccharides, nucleic acids, lipids and fats. To highlight the spectral features, Fig. 2 shows second derivative of the mean spectra in the 1800–950 cm^{-1} absorption region, corresponding to the normal tissue (Fig. 2A) and three different pathological situations encountered during surgery (2B: tissue from a patient with an aortic bicuspid valve; 2C: aneurismal tissues from patients with a normal (tricuspid) valve; 2D: aneurismal tissues from patients with an aortic bicuspid valve). Specific regions have been identified [9,10] corresponding to Amide I and II bands, respectively, centred near 1650 and 1545 cm^{-1} ; the regions between 1050 and 1450 cm^{-1} also contain additional vibrational information about proteins and significant contributions of collagen appear at 1080, 1205 and 1340 cm^{-1} . It can be noted that the spectrum displayed in Fig. 2B, corresponding to a tissue originating from a patient with an aortic bicuspid valve, exhibits an additional

marked peak at 1740 cm^{-1} , assigned to an ester carbonyl, which could be from cholesterol esters. This appears quite peculiar because one would expect to see presence of cholesterol esters peak in cases of aneurysm and not in that of bicuspid aortic valve. However, it must be pointed out that this assignment is based on the fact that this particular patient had a very high cholesterol level and that the presence of this peak cannot systematically be assigned to aneurysms and presence of atheroma.

The spectral window contains other interesting features and reveals some marked differences on the structural conformation of proteins [11,12]. The absorption band in the 1667–1643 cm^{-1} region represents alpha helical structure whereas the band comprised between 1642 and 1628 cm^{-1} can be assigned to beta-sheet secondary structure.

3.1. Analysis of the spectral information contained in IR images

One of the advantages of spectral images is that they contain both chemical and spatial information. The rapidity of modern IR imaging makes it possible to generate images from large tissue sizes and the richness of the spectral information contained makes it an interesting *in vitro* method to study the changes between healthy and pathological specimens [13]. However, the generation of an increasing number of spectra (reaching several thousands in some cases) via such approach which needs to be treated, makes the task more and more difficult. In this study we have analysed our data using two different approaches based either on a univariate (band ratio or specific spectral window) or on a multivariate method (principal components analysis, PCA).

From the information observed in the comparison of mean spectra or their second derivatives, IR images have been built using the band area ratio 1445–1335/1700–1485 cm^{-1} . In order to compare the tissue types, these images have been scaled to the same intensity. As can be seen in Fig. 3A, the spectral image corresponding to a normal tissue exhibits a very flat and quite homogeneous profile. On the other hand, the diseased tissue carrying an aneurysm shows a very inhomogeneous profile (Fig. 3B). Using this 3D representation of spectral images, new light can be shed on a doubtful case or a surgical dilemma such as that of a patient with a bicuspid aortic valve. This is demonstrated in Fig. 3C, where the profile obtained is intermediate and tends to indicate that this tissue already shows early characteristics of a pathological situation. Recent studies have demonstrated that bicuspid aortic valve is related to genetic matrix and elastin disorders probably also implied in some ascending aortic dilations and aneurysms [3,14,15]. Thus, this type of approach is interesting and can be helpful for diagnostic purposes since it can give complementary information on the nature of the tissue that is difficult to appraise by histopathology.

Another way of exploiting the data contained in a spectral image can be via band ratio analysis. From the derivative spectra, we observed differences in the protein absorbing region in the range 1667–1643 cm^{-1} and 1642–1628 cm^{-1}

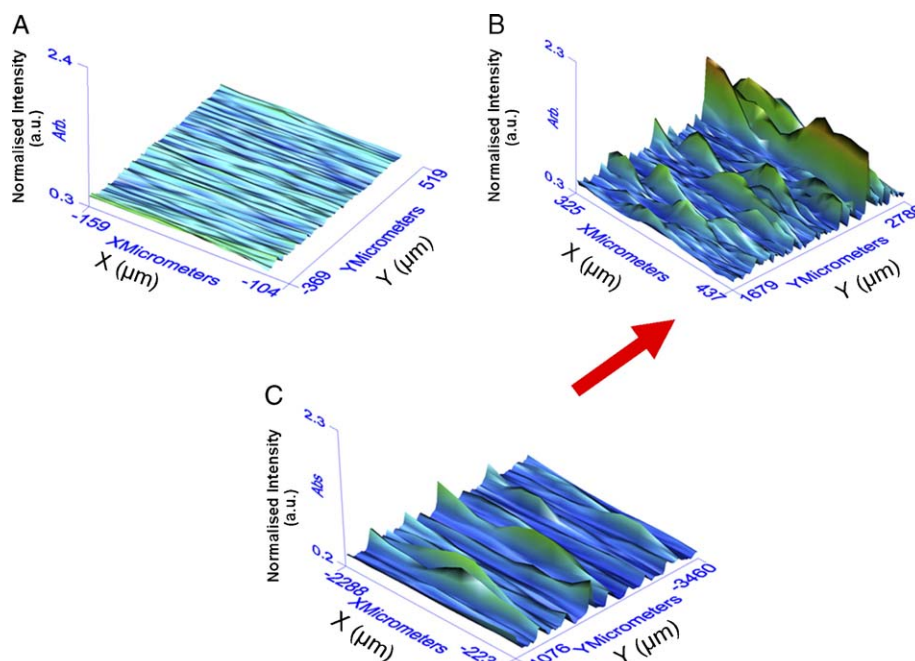


Fig. 3. 3D visualisation showing spectral images built on the band ratio $1445\text{--}1335/1700\text{--}1485\text{ cm}^{-1}$ of FT-IR spectra. The first band includes mainly the CH vibrations of proteins while the second region corresponds to their C=O and N-H modes (Amide I and II respectively). For a better comparison, all images have been scaled to the same intensity. The healthy tissue shows a flat and homogeneous profile (A) while the aneurismal tissue exhibits a more inhomogeneous appearance (B). The tissue corresponding to a bicuspid aortic valve shows a tendency which is intermediate (C) indicating early signs of a pathological situation.

corresponding respectively to alpha-helical and beta-sheet secondary structures. Since tissue modification and consequently the associated aortic pathology is related to the degradation of the fibrous proteins (collagen and elastin) of the different tissues, we have used the ratio of these two bands ($R = 1667\text{--}1643\text{ cm}^{-1}/1642\text{--}1628\text{ cm}^{-1}$) present in the protein absorption region to monitor the changes within each tissue type. The calculation of this band ratio was carried out for each spectrum across a line following the cross section of the

tissue, from the intima to the adventice, and the average and standard deviation were evaluated. For each tissue type, ten different lines were calculated and the results are presented in the form of histograms in Fig. 4. This allows to compare the evolution of protein structure in relation with tissue type. Three distinguished groups came out of this analysis: tissue from patient with a bicuspid aortic valve is represented by a very low ratio ($R < 2$); those from healthy patients with an average value ($R \sim 4$), and the two groups containing

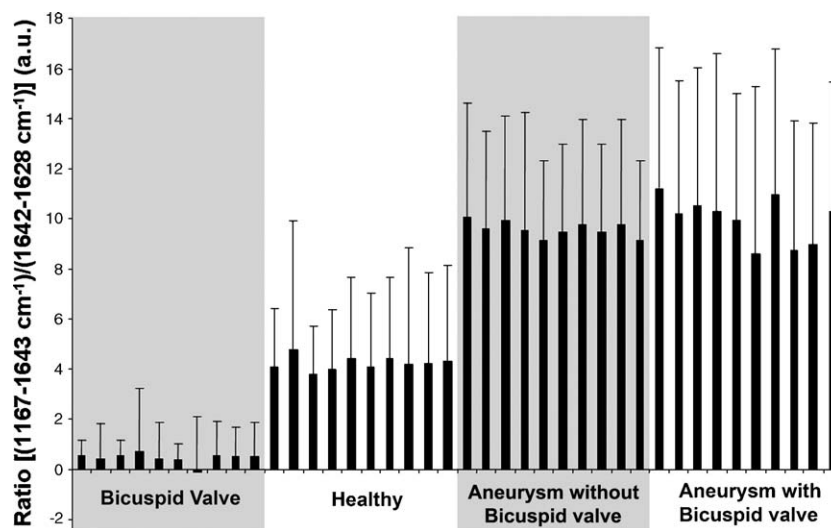


Fig. 4. Histogram of the band area ratio ($R = 1667\text{--}1643\text{ cm}^{-1}/1642\text{--}1628\text{ cm}^{-1}$) for the four tissue types, calculated from second derivative spectra. Each bar represents the average value of R calculated for each spectrum along a line through the tissue cross section from the intima to the adventice. For each tissue type, 10 cross sections were calculated. We note that due to sample preparation, holes and kinks can appear in the tissues and consequently some points can give aberrant values of R . These have been omitted in this calculation.

aneurismal patients with and without a bicuspid valve exhibiting higher values of this ratio ($R \sim 10$). We point out that due to sample preparation, holes and kinks can appear in the tissues and consequently some points can give aberrant values of R . These have been omitted from this calculation and not presented. This analysis shows that healthy aorta presents a value near 4 and can be considered as a reference for comparison with different pathological tissues. Other tissue types fall either below or above this reference value.

Collagen and elastin fibrous proteins constitute the most important components of the aortic wall. Collagen is composed principally of alpha helix while elastin is made essentially of beta sheets secondary structures [16–18]. Consequently, a variation in collagen or elastin content (or both) can be directly associated with modifications in the spectral profile of bands representative of alpha and beta structures. Bicuspid aortic valve is a congenital malformation which can be associated with a particular structure of the aortic wall. By inspecting the second derivative spectra of this tissue (data not shown), we noticed that the band corresponding to beta structures ($1642\text{--}1628\text{ cm}^{-1}$) remained constant while that of alpha helical structure ($1667\text{--}1643\text{ cm}^{-1}$) decreased. In the case of patient with aortic bicuspid valves, the decrease of the band assigned to alpha structure can be associated to a collagen depletion in the aortic wall.

Compared to healthy tissues, aneurismal tissues (with or without bicuspid valves) present similar band intensities for alpha helix type structure. So, collagen structure seems to be equally present. The difference appears in bands in the $1642\text{--}1628\text{ cm}^{-1}$ region. The decrease in beta structures in such tissues indicates elastin depletion or simply a modification of elastin structure in relation with the aneurysm development [19,20], which causes a loss of parallelism in this artery wall making it less elastic and more fragile.

Comparison of tissue specimens from aortic bicuspid valves and aneurysm with aortic bicuspid valves shows a strong increase in alpha structure between these two types of pathologies. A plausible explanation could be a reaction of the body against the development of a pathological situation in the form of a synthesis of collagen to consolidate the aortic wall.

3.2. Multivariate analysis of spectral information using PCA

Principal components analysis (PCA) is a powerful and objective tool that has been successfully used as an effective approach to visualise and to mine information from data tables with a large number of variables such as those contained in FTIR spectra. The discriminant information can then be helpful to differentiate various pathological situations in cell and tissue investigations [21,22]. The advantage of PCA over univariate methods is that it can look for the maximum variance in a large data set by comparing all the absorption wavelengths. In order to optimise the discrimination between the different tissue types, we used second derivative spectra as input for the PCA. The frequency range between $950\text{ and }1750\text{ cm}^{-1}$, containing not only collagen and elastin main absorption peaks the principal proteins that constitute the arteries wall, but also

other macromolecules, was used for the chemometric evaluation. Six tissue specimens were analysed and characterised as follows: 1 healthy tissue, tissue of 1 patient with aortic bicuspid valve, aneurismal tissues from 2 patients without aortic bicuspid valve, and aneurismal tissues from 2 patients with aortic bicuspid valve. Our first goal was to evaluate the possibility of discriminating tissues of healthy patient from those with different pathologies by using the PCA approach. The 2D-scatter plot displayed in Fig. 5 shows that by using the two first principal components, three distinct clusters could be obtained. The first cluster is composed of mean derivative spectra from the healthy tissue, the second cluster groups those obtained from a patient with bicuspid aortic valve, and the last cluster contained those from the remaining 4 cases corresponding to aneurismal tissues from patients with or without aortic bicuspid valves. The first loading vector or PC1 accounts for 33% of the explained variance and permits to discriminate healthy from pathological tissues. PC2 accounts for 28% of the explained variance and allows separating tissues with aortic bicuspid valves. As can be seen, the plot of PC1 versus PC2 offers a good discrimination of spectra of the different tissue types without any outliers. Modification in aortic structure due to genetics pattern or modification of blood pressure could explain the structural differences observed in the tissues. From a spectroscopic point of view, tissues of patients with aortic bicuspid valves seem to be not normal although their aortic diameter is normal. Patients with aortic bicuspid valves present aortic structural modifications associated with valve malformation. However, this aortic wall modification is not considered as pathological because of the absence of aortic dilation but rather as a predisposition to future aneurysm development. This is an

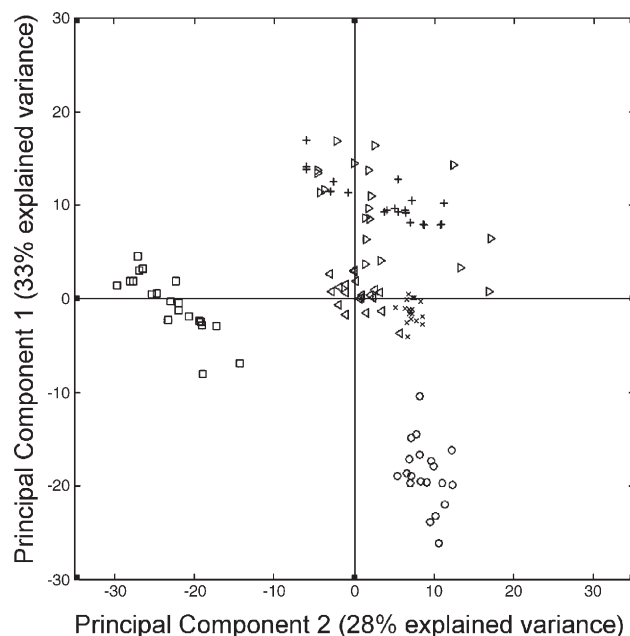


Fig. 5. Discrimination of six different aorta tissues by Principal Component Analysis method. Components 1 and 2 of second derivative of infrared spectra over the range $950\text{--}1750\text{ cm}^{-1}$ were used to define 2D space representations. O: healthy, □: aortic bicuspid valves, ▷ and ◁: aneurysms without bicuspid valve, + and x: aneurysms associated to aortic bicuspid valve.

interesting aspect because the spectroscopic method shows the potential to reveal biochemical alterations in tissues even before diagnosis of the disease, which is here based on the molecular and morphological changes of the main constituents of the aortic tissue. The second objective was to differentiate between aneurysms with or without bicuspid valves. This was more difficult as was also the case using band ratio analysis. Therefore, results on band ratio and PCA analyses confirm this observation. An important observation in this study is that FTIR spectroscopic data give 2 distinct groups of non dilated tissues (healthy and patient with aortic bicuspid valve) which seem to form a single group with the advent of an aneurysm.

4. Conclusion

Over the last few years, FTIR microspectroscopy and imaging has improved in both rapidity and performance as an analytical tool. It is suitable for in vitro investigation of healthy and pathological tissues since it combines both spatial and chemical information. In this study we have shown that the spectral images can be interpreted using different approaches based on either univariate or multivariate methods. Three-dimensional representation using absorbance values, after pre-processing of data, could be one way of visualising spectral images in view of recognising healthy from aneurysmal tissues and can also show the trend of suspected tissues. Using simple band ratio such as alpha-helical to beta-sheet content and multivariate analysis like PCA, the spectral information contained in the IR images can be used to characterise tissues with aortic diseases like aneurysmal dilations. Moreover, this approach highlights tissue composition differences between non dilated aortic tissues from patients with tricuspid or bicuspid aortic valves. Spectral modifications seem to be strongly correlated to collagen and elastin conformational modifications. However, the importance of the contribution of these proteins in each tissue category needs to be clearly established. This preliminary study based on a limited number of samples will be completed by increasing the recruitment of biopsies for each tissue type.

References

- [1] E. Arteaga-Solis, B. Gayraud, F. Ramirez, Elastic and collagenous networks in vascular diseases, *Cell Struct. Funct.* 25 (2000) 69–72.
- [2] H. Nagase, J.F. Woessner Jr., Matrix metalloproteinases, *J. Biol. Chem.* 274 (1999) 21491–21494.
- [3] C.M. Dollery, J.R. McEwan, A.M. Henney, Matrix metalloproteinases and cardiovascular disease, *Circ. Res.* 77 (1995) 863–868.
- [4] T. Taketani, Y. Imai, T. Morota, K. Maemura, H. Morita, D. Hayashi, T. Yamazaki, R. Nagai, S. Takamoto, Altered patterns of gene expression specific to thoracic aortic aneurysms: microarray analysis of surgically resected specimens, *Int. Heart J.* 46 (2005) 265–277.
- [5] D. Bonderman, E. Gharehbaghi-Schnell, G. Wollenek, G. Maurer, H. Baumgartner, I.M. Lang, Mechanisms underlying aortic dilatation in congenital aortic valve malformation, *Circulation* 99 (1999) 2138–2143.
- [6] D.M. Milewicz, K. Michael, N. Fisher, J.S. Coselli, T. Markello, A. Biddinger, Fibrillin-1 (FBN1) mutations in patients with thoracic aortic aneurysms, *Circulation* 94 (1996) 2708–2711.
- [7] G.B. Luciani, G. Casali, G. Faggian, A. Mazzucco, Predicting outcome after reoperative procedures on the aortic root and ascending aorta, *Eur. J. Cardio-thorac Surg.* 17 (2000) 602–607.
- [8] A. Avolio, D. Jones, M. Tafazzoli-Shadpour, Quantification of alterations in structure and function of elastin in the arterial media, *Hypertension* 32 (1998) 170–175.
- [9] J.M. Gentner, E. Wentrup-Byrne, P.J. Walker, M.D. Walsh, Comparison of fresh and post-mortem human arterial tissue: an analysis using FT-IR microspectroscopy and chemometrics, *Cell. Mol. Biol. (Noisy-le-Grand)* 44 (1998) 251–259.
- [10] C.S. Colley, S.G. Kazarian, P.D. Weinberg, M.J. Lever, Spectroscopic imaging of arteries and atherosclerotic plaques, *Biopolymers* 74 (2004) 328–335.
- [11] C.C. Orfanidou, S.J. Hamodrakas, G.D. Chryssikos, E.I. Kamitsos, S.E. Wellman, S.T. Case, Spectroscopic studies of *Manduca sexta* and *Sesamia nonagrioides* chorion protein structure, *Int. J. Biol. Macromol.* 17 (1995) 93–98.
- [12] L. Debelle, A.J. Alix, M.P. Jacob, J.P. Huvenne, M. Berjot, B. Sombret, P. Legrand, Bovine elastin and kappa-elastin secondary structure determination by optical spectroscopies, *J. Biol. Chem.* 270 (1995) 26099–26103.
- [13] L. Debelle, A.J. Alix, The structures of elastins and their function, *Biochimie* 81 (1999) 981–994.
- [14] P.W. Fedak, M.P. de Sa, S. Verma, N. Nili, P. Kazemian, J. Butany, B.H. Strauss, R.D. Weisel, T.E. David, Vascular matrix remodeling in patients with bicuspid aortic valve malformations: implications for aortic dilatation, *J. Thorac. Cardiovasc. Surg.* 126 (2003) 797–806.
- [15] D. Pacini, L. Di Marco, A. Loforte, E. Angeli, A. Dell'amore, M. Bergonzini, R. Di Bartolomeo, Reoperations on the ascending aorta and aortic root. Early and late results? *J. Cardiovasc. Surg. (Torino)* 46 (2005) 491–498.
- [16] A. Tfayli, O. Piot, A. Durlach, P. Bernard, M. Manfait, Discriminating nevus and melanoma on paraffin-embedded skin biopsies using FTIR microspectroscopy, *Biochim. Biophys. Acta* 1724 (2005) 262–269.
- [17] K.F. Smith, P.I. Harris, D. Chapman, K.B. Reid, S.J. Perkins, Beta-sheet secondary structure of the trimeric globular domain of C1q of complement and collagen types VIII and X by Fourier-transform infrared spectroscopy and averaged structure predictions, *Biochem. J.* 301 (Pt. 1) (1994) 249–256.
- [18] D. Wetzel, G. Post, R. Lodder, Synchrotron infrared microscopic analysis of collagens I, III and elastin on the shoulders of human thin-cap fibroatheromas, *Vib. Spectrosc.* 38 (2005) 53–59.
- [19] F.H. Silver, I. Horvath, D.J. Foran, Viscoelasticity of the vessel wall: the role of collagen and elastic fibers, *Crit. Rev. Biomed. Eng.* 29 (2001) 279–301.
- [20] T. Savunen, H.J. Aho, Annulo-aortic ectasia. Light and electron microscopic changes in aortic media, *Virchows Arch. A: Pathol. Anat. Histopathol.* 407 (1985) 279–288.
- [21] C. Murali Krishna, G. Kegelaer, I. Adt, S. Rubin, V.B. Kartha, M. Manfait, G.D. Sockalingum, Characterisation of uterine sarcoma cell lines exhibiting MDR phenotype by vibrational spectroscopy, *Biochim. Biophys. Acta* 1726 (2005) 160–167.
- [22] A.M. Nilsson, D. Heinrich, J. Olajos, S. Andersson-Engels, Near infrared diffuse reflection and laser-induced fluorescence spectroscopy for myocardial tissue characterisation, *Spectrochim. Acta, A Mol. Biomol. Spectrosc.* 53A (1997) 1901–1912.